Title: A Bayesian Framework for Multiple Trait Colocalization from Summary Association Statistics

Claudia Giambartolomei[1], Jimmy Zhenli Liu[2], Wen Zhang[3], Mads Hauberg[3,4], Huwenbo Shi[5], James Boocock[1], Joe Pickrell[2], Andrew E. Jaffe[6], the CommonMind Consortium[#], Bogdan Pasaniuc*[1], Panos Roussos*[3,7,8]

[1]Department of Pathology and Laboratory Medicine, University of California, Los Angeles, Los Angeles, CA 90095, USA; Department of Human Genetics, University of California, Los Angeles, Los Angeles, CA 90095, United States of America.
[2] New York Genome Center, New York, New York, United States of America
[3]Department of Genetics and Genomic Science and Institute for Multiscale Biology, Icahn School of Medicine at Mount Sinai, New York, New York, 10029, United States of America.
[4]The Lundbeck Foundation Initiative of Integrative Psychiatric Research (iPSYCH), Aarhus University, Aarhus, 8000, Denmark.
[5]Bioinformatics Interdepartmental Program, University of California, Los Angeles, 90024
[6]Lieber Institute for Brain Development, Johns Hopkins Medical Campus; Departments of Mental Health and Biostatistics, Johns Hopkins Bloomberg School of Public Health Baltimore, MD, 21205, United States of America.
[7]Department of Psychiatry and Friedman Brain Institute, Icahn School of Medicine at Mount Sinai, New York, New York, 10029, United States of America.
[8]Mental Illness Research Education and Clinical Center (MIRECC), James J. Peters VA Medical Center, Bronx, New York, 10468, United States of America.

The members of the CommonMind Consortium are listed under “Consortia”.

Correspondence:
Dr. Panos Roussos
Icahn School of Medicine at Mount Sinai
Department of Psychiatry and Department of Genetics and Genomic Science and Institute for Multiscale Biology
One Gustave L. Levy Place,
New York, NY, 10029, USA
Panagiotis.roussos@mssm.edu

Dr. Claudia Giambartolomei
University of California, Los Angeles, Los Angeles
Department of Pathology and Laboratory Medicine,
Los Angeles, CA 90095, USA
claudia.giambartolomei@gmail.com

ABSTRACT

Most genetic variants implicated in complex diseases by genome-wide association studies (GWAS) are non-coding, making it challenging to understand the causative genes involved in disease. Integrating external information such as quantitative trait locus (QTL) mapping of molecular traits (e.g., expression, methylation) is a powerful approach to identify the subset of GWAS signals explained by regulatory effects. In particular, expression QTLs (eQTLs) help pinpoint the responsible gene among the GWAS regions that harbor many genes, while methylation QTLs (mQTLs) help identify the epigenetic mechanisms that impact gene expression which in turn affect disease risk. In this work we propose **m**ultiple-trait-c**oloc** (***moloc***), a Bayesian statistical framework that integrates GWAS summary data with multiple molecular QTL data to identify regulatory effects at GWAS risk loci. We applied ***moloc*** to schizophrenia (SCZ) and eQTL/mQTL data derived from human brain tissue and identified 52 candidate genes that influence SCZ through methylation. Our method can be applied to any GWAS and relevant functional data to help prioritize disease associated genes.

INTRODUCTION

Genome-wide association studies (GWAS) have successfully identified thousands of genetic variants associated with complex diseases[1]. However, since the discovered associations point to non-coding regions, it is difficult to identify the causal genes and the mechanism by which risk variants mediate disease susceptibility. Advancement of high-throughput array and sequencing technology has enabled the identification of quantitative trait loci (QTLs), genetic variants that affect molecular phenotypes such as gene expression (expression QTL or eQTL) and DNA methylation (methylation QTL or mQTL). Integration of molecular QTL data has the potential to functionally characterize the GWAS results. Additionally, analyzing two datasets jointly has been a successful strategy to identify shared genetic variants that affect different molecular processes, in particular eQTL and GWAS[2–5] and mQTL and GWAS[6–9] integration. All these previous efforts have focused on pairwise trait integration (e.g. eQTL and GWAS or mQTL and GWAS). Analyzing multiple datasets jointly has the potential to increase power for functional characterization of non-coding, risk variants. In addition, it has the potential to link changes in methylation with specific transcripts, avoiding the issues of arbitrary annotating GWAS-mQTL associations to the nearby genes.

To our knowledge, a statistical approach to integrate multiple QTL datasets with GWAS is lacking. Therefore, we developed **m**ultiple-trait-**coloc** (***moloc***), a statistical method to quantify the evidence in support of a common causal variant at a particular risk region across multiple traits. We applied *moloc* to schizophrenia (SCZ), a complex polygenic psychiatric disorder, using summary statistics from the most recent and

largest GWAS by the Psychiatric Genomics Consortium[10], which reported association for 108 independent genomic loci. eQTL data were derived from the CommonMind Consortium[2], which generated the largest eQTL dataset in the dorsolateral prefrontal cortex (DLPFC) from SCZ cases and control subjects (N=467). Finally, we leveraged mQTL data that were previously generated in human DLPFC tissue (N=121) to investigate epigenetic variation in SCZ[6]. Integration of multiple phenotypes helps better characterize the genes predisposing to complex diseases such as SCZ.

MATERIALS AND METHODS

Overview of the Method

We introduce an approach (***moloc***) to detect colocalization among any number of traits concurrently rather than pairwise colocalizatin (i.e. ***coloc***[11]) . We first derive our model using three traits, then generalize to any number of traits. The input of the model is the set of summary statistics derived from three traits measured in distinct datasets of unrelated individuals, {1} GWAS (which we denote as G), {2} eQTL (E) and {3} mQTL (M). We define a genomic region containing **Q** variants, for example a *cis* region around expression or methylation probe. We are interested in a situation where summary statistics (effect size estimates and standard errors) are available for all datasets in the genomic region. If we consider three traits, there can be up to three causal variants and 15 possible scenarios summarizing how the variants are shared among the traits. Each hypothesis can be represented by a set of index set according to which of the traits each SNP is associated with: H_0- no association to any trait, H_1- association only for trait {1}, H_2- association only for trait {2}, H_3- association only for trait {3}, H_4-

association for traits {1 and 2}, H_5- association for traits {2 and 3}, H_6- association for traits {1 and 3}, H_7- association for trait 1 and 2, but different causal variants for {1} and {2}, H_8- association for traits 2 and 3, but different causal variants for {2} and {3}, H_9- association for traits 1 and 3, but different causal variants for {1} and {3}, H_{10}- association for traits 1, 2 and 3, but different causal variants for {1} and {2,3}, H_{11}- association for traits 1, 2 and 3, but different causal variants for {3} and {1,2}, H_{12}- association for traits 1, 2 and 3, but different causal variants for {2} and {1,3}, H_{13}- association for traits 1, 2 and 3, but different causal variants for {1}, for {2} and for {3}, and H_{14} SNP is associated with all 3 traits (GEM).

Our aim is to find the evidence supporting 15 possible scenarios $(H_0 \cdots H_{14})$, of sharing of SNPs among traits in the given genomic region. We compute the posterior probability of a configuration by weighting the likelihood of the data *D* given a configuration *S*, *P(D|S)*, by the prior probability of a configuration, *P(S)*. We obtain Bayes factors by dividing each likelihood to the baseline likelihood supporting the first model of no association with any trait H_0. The Regional Bayes Factor (RBF) is then the sum over all configurations *Sh* which are consistent with the given hypothesis:

$$RBF_h = \frac{P(H_h|D)}{P(H_0|D)} = \sum_{S \in S_h} \frac{P(D \mid S)}{P(D \mid S_0)} \times \frac{P(S)}{P(S_0)}, \qquad (1)$$

where, *P(D|S)/P(D|S₀)* is the Bayes Factor for each configuration compared to the baseline configuration of no association with any trait *S₀*, *P(S)/P(S₀)* is the prior odds of a configuration compared with the baseline configuration *S₀*, and the sum is over Sh, the set of configurations supporting hypothesis $H_0$to H_{14}. Similar to pairwise

colocalization[11] we then estimate the evidence in support of different scenarios in a given genomic region using the posterior probability supporting hypothesis *h* among *H* possible hypothesis, is computed from:

$$PP_h = P(H_h|D) = \frac{P(H_h|D)}{\sum_{i=0}^{H} P(H_i)} = \frac{\frac{P(H_h|D)}{P(H_0|D)}}{1 + \sum_{i=1}^{H} \frac{P(H_i|D)}{P(H_0|D)}} \qquad (2)$$

Therefore, in our application, the algorithm outputs 15 posterior probabilities. We are most interested in the scenarios supporting a shared causal variant for two and three traits. All the computations are analytical and no iterative methods are required.

We make three important assumptions in *moloc*, the same that are made in our previous *coloc* methodology. Firstly, that the causal variant is included in the set of *Q* common variants, either directly typed or well imputed. If the causal SNP is not present, the power to detect a common variant will be reduced depending on the linkage disequilibrium (LD) between other SNPs included in the model and the causal SNP (**Figure S5**). Secondly, we assume at most one causal variant is present for each trait. In the presence of multiple causal variants per trait, this algorithm is not able to identify colocalization between additional association signals independent from the primary one. Thirdly, as we do not explicitly model LD between SNPs, we assume the samples are drawn from the same ethnic population and therefore have identical allele frequencies and patterns of LD.

Configurations and Notations

To compute the likelihood of the data, we need to first introduce the concepts of configurations and sets of configurations supporting each hypothesis listed above. Each trait at a region of *Q* variants can be described using a binary vector of (0,1) values, where a 1 means that the SNP is associated with the trait and only 1 SNP is non-zero. We call a configuration ***S*** a possible combination of ***M*** binary vectors, an array with dimensions *Q* X *M*, where *M* is the number of traits. The columns represent a particular sharing of any one SNP across the traits. We can combine the configurations into sets corresponding to different scenarios of SNP sharing to assess the evidence in support of each model. Thus, each hypothesis can be represented by a set of index set containing the traits each causal SNP associates with.

To illustrate our notation, consider a region with 8 SNP. Four examples of configurations are show in **Figure 1**. The "." in the subscript denotes scenarios supporting different causal variants. For instance, GE summarizes the scenario for one causal variant shared between traits GWAS and eQTL (**Figure 1** - Right plot top panel); GE.M summarizes the scenario with one causal variant for traits GWAS and eQTL, and a different causal variant for trait mQTL (**Figure 1** - Left plot bottom panel).

Formally, let Sh denote the set of configurations supporting hypothesis h, then Sh can be written as:

$$S_h = \left\{ \cup_{k=1}^{|h|} \left\{ i_{|h|} \right\} \times h_k \mid \forall\, i_1 ... i_{|h|} \in \{1, ..., Q\}, i_1 \neq \cdots \neq i_{|h|} \right\}, \qquad (3)$$

where hk represents the k-th element (an index set) in the set representation of the hypothesis h.

We can then assess the support for each hypothesis by assigning the possible combinations of causal configurations (binary vectors with at most 1 entry equal to 1) to one of the following 15 hypotheses listed above.

Bayes Factor of a SNP with one trait

We start by computing a Bayes Factor for each SNP and each of the trait (i.e GWAS, eQTL, mQTL). We assume a simple linear regression model to relate the phenotypes or a log-odds generalized linear model for the case-control dataset, and the genotypes. Using the Wakefield Approximate Bayes factors[12] (WABF), only the variance and effect estimates from regression analysis are needed, as shown below and previously described[11,13]:

$$WABF_i^j = \frac{1}{\sqrt{1-r}} \times exp\left[-\frac{Z_i^{2(j)}}{2} \times r\right] \quad (4)$$

where Zij = βˆ/√V is the usual Z statistic and the shrinkage factor r is the ratio of the variance of the prior and total variance (r = W/(V + W)).

The WABF requires specifying the variance W of the normal prior. In the moloc method we set W to 0.15 for a continuous trait and 0.2 for the variance of the log-odds ratio parameter, as previously described [11]. Another possibility is to average over Bayes factors computed with W = 0.01, W = 0.1, and W = 0.5 [14]. We provide this as an option that can be specified by the user.

If the variance of the estimated effect size V is not provided, it can be approximated using the allele frequency of the variant f, the sample size N (and the case control ratio

s for binary outcome). For example, in the case-control setting, V is estimated using the following equation[11]:

$$V_i = Var(\hat{\beta}_i) = \frac{1}{Ns_i(1-s_i) \times 2f_i(1-f_i)} \quad (5)$$

Bayes factor of a SNP across more than one trait

To compute the BF where a SNP i associates with more than one trait, we use:

$$BF_{i,\mathbf{s}} = \prod_{j \in S} WABF_i^j \quad (6)$$

Where **s** is the set of trait indices for which SNP i is associated with.

Note that the computations under >1 trait multiply the individual Bayes Factors together. This is equivalent to the Bayes Factor under the maximum heterogeneity model used in Wen and Stephens[15]. Two key assumptions are necessary for the following computations. Firstly that the traits are measured in unrelated individuals, and secondly that the effect sizes for the two traits are independent. We will consider when these assumptions are appropriate in Discussion.

Prior probabilities that SNP i associates with traits in s

The prior probability that SNP i associates with all traits indexed in a set in our three trait model is: π_{φ}SNP i associates with no trait, with one trait, pairs or traits or all traits $\pi_{\{1,2,3\}}$ such that they sum to 1: $\pi_{\varphi} + \pi_{\{1\}} + \pi_{\{2\}} + \pi_{\{3\}} + \pi_{\{1,2\}} + \pi_{\{1,3\}} + \pi_{\{2,3\}} + \pi_{\{1,2,3\}} = 1$

Prior Probabilities of each configuration

In our model (Equation 1), *P(S)* is the prior probability of a configuration. We can define these priors from the prior probability that a SNP i associates with traits indexed in π_s (section above). Additionally, since the prior probability *P(S)* of any one configuration in the different sets do not vary across SNPs that belongs to the same set S_h, we can multiply the likelihoods by one common prior supporting the different hypothesis[11]. P(S) depends on a ratio of π_s and on Q, the number of SNPs in the region. Specifically, the prior probability of the configuration associated with no traits is $P_0 = \pi_{\varphi}^{Q}$, with one trait is e.g. $P_1 = Q \times \pi_0^{Q-1}\pi_{\{1\}}$, with a pair of traits with a causal variant shared by trait {1} and {2} is e.g. $P_4 = Q \times \pi_0^{Q-1}\pi_{\{1,2\}}$, with a pair of traits with a different causal variant for trait {1} and {2} is e.g. $P_7 = Q(Q-1) \times \pi_0^{Q-2}\pi_{\{1\}}\pi_{\{2\}}$, and with all three traits, each with a different causal variant is $P_{13} = Q(Q-1)(Q-2) \times \pi_0^{Q-3}\pi_{\{1\}}\pi_{\{2\}}\pi_{\{3\}}$.

Regional Bayes factor (the 3-trait special case)

The Regional Bayes Factor (RBF) can be computed by summing the probability of all the causal configurations consistent with a particular hypothesis (Equation 1).

For example, the RBF for hypothesis 4 is:

- $RBF_4 = \frac{P(H_4|D)}{P(H_0|D)} = \pi_{\{1,2\}} \times \sum_{i=1}^{Q} BF_{i,\{1,2\}} = \pi_{\{1,2\}} \times \sum_{i=1}^{Q} WABF_i^1 WABF_i^2$

For example, the RBF for hypothesis 11 is:

- $RBF_{11} = \frac{P(H_{11}|D)}{P(H_0|D)} = \pi_{\{3\}} \times \pi_{\{1,2\}} \times \sum_{i=1}^{Q}\sum_{j=1}^{Q} BF_{i,\{3\}}BF_{j,\{1\}}BF_{j,\{2\}}$
  $= \pi_{\{3\}} \times \pi_{\{1,2\}} \times \sum_{i=1}^{Q}\sum_{j=1}^{Q} WABF_i^3 WABF_j^1 WABF_j^2 I[i \neq j]$

where WABF are Wakefield's Asymptotic Bayes Factors for each SNP and each trait 1, 2 and 3,I[i ≠ j] is an indicator that evaluates to 1 if SNP i and j are different and to 0 otherwise, π are the prior probabilities that SNP i is the causal SNP under a specific model.

Notably, the RBF for non-colocalized signals [7 . . . n − 1] can be derived from the colocalized signals. This generalization speeds up computation significantly:

- $\frac{P(H_{11}|D)}{P(H_0|D)} = \pi_{\{3\}} \times \pi_{\{1,2\}} \times \sum_{i=1}^{Q} BF_{i,\{3\}} \sum_{j=1}^{Q} BF_{j,\{1,2\}} - \left[\frac{\pi_{\{3\}} \times \pi_{\{1,2\}}}{\pi_{\{1,2,3\}}} \times \frac{P(H_{14}|D)}{P(H_0|D)} \right]$

In practice, we collapsed the prior probabilities to a smaller set for each kind of configuration. We set the prior probability that a SNP is causal in each trait to be identical (π{1} = π{2} = π{3}) and refer to this a p1. We also set the prior probability that is associated with two traits to be identical (π{1,2},π{2,3},π{1,3}) and refer to this as p2. We refer to the prior probability that SNP i the causal for all traits (π{1,2,3}) as p3.

Regional Bayes factor (the general case)

Across a set of M traits {1,2,3...,M}, for a hypothesis h, where there are more than one independent associations among the M traits (i.e. |h| > 1), we can compute the Regional Bayes factor supporting h using a generalization which speeds up computation significantly:

$$RBF_h = \frac{P(H_h|D)}{P(H_0|D)} = \prod_{s \in h} \pi_s \sum_{i=1}^{Q} BF_{i,s} - \frac{\prod_{s \in h} \pi_s}{\pi_t} \sum_{i=1}^{Q} \pi_t BF_{i,t}, \qquad (7)$$

where **s** is the set of trait indices for which SNP i is associated with, and **t** is the union of the index set in ***h***, i.e. $t = \cup_{j=1}^{|h|} h_j$.

For example, let there be three traits {1,2,3} with two independent associations. The first signal colocalizes with traits 1 and 2 while the second is an independent association with trait 3. Hence, M = 3, h = {1,2},{3} and:

$$\frac{P(H_h|D)}{P(H_0|D)} = \pi_{\{1,2\}}\pi_{\{3\}} \sum_{i=1}^{Q} BF_{i\{1,2\}} \sum_{j=1}^{Q} BF_{j\{3\}} - \frac{\pi_{\{1,2\}}\pi_{\{3\}}}{\pi_{\{1,2,3\}}} \sum_{i=1}^{Q} \pi_{\{1,2,3\}} BF_{i\{1,2,3\}}$$

We pre-compute the single terms in the above equation, so that in practice we have:

$$\frac{P(H_h|D)}{P(H_0|D)} = RBF_{\{1,2\}} \times RBF_{\{3\}} - \frac{\pi_{12} \times \pi_3}{\pi_{123}} \times RBF_{\{1,2.3\}}$$

Similarly, let there be five traits {1,2,3,4,5} with two independent associations. First one is common to traits 1, 2, the second one common to traits 4 and 5. Hence, M = 5, h = {{1, 2}, {4, 5}} and:

$$\frac{P(H_h|D)}{P(H_0|D)} = \pi_{\{1,2\}}\pi_{\{4,5\}} \sum_{i=1}^{Q} BF_{i\{1,2\}} \sum_{j=1}^{Q} BF_{j\{4,5\}} - \frac{\pi_{\{1,2\}}\pi_{\{4,5\}}}{\pi_{\{1,2,4,5\}}} \sum_{i=1}^{Q} \pi_{\{1,2,4,5\}} BF_{i\{1,2,4,5\}}$$

GWAS dataset

Summary statistics for genome-wide SNP association with Schizophrenia were obtained from the Psychiatric Genomics Consortium-Schizophrenia Workgroup (PGC-SCZ) primary meta-analysis (35,476 cases and 46,839 controls) [10].

Expression QTL (eQTL) analysis

For the eQTL associations, we used pre-QC'ed expression and imputed genotypes, on case-control of European-ancestry (N=467) collected by the CommonMind Consortium. Briefly, gene expression was assayed data from post-mortem DLPFC (Brodmann areas 9 and 46) with RNA-seq and mapped to human Ensembl gene reference (v70) using TopHat version 2.0.9 and Bowtie version 2.1.0. Genes with less than 1 CPM (counts per million) in at least 50% of the samples were discarded and RNA-seq data for a total of 16,423 Ensembl genes were considered for downstream analyses. After RNA sample QC, and retaining only genetically-identified European-ancestry individuals, a total of 467 samples were used for downstream analyses. These comprised 209 SCZ cases, 52 AFF (Bipolar, Major depressive disorder, or Mood disorder, unspecified) cases, and 206 controls. The expression data was voom-adjusted for both known covariates (RIN, library batch effect, institution, diagnosis, post-mortem interval, age and sex) and hidden confounds identified based on surrogate variable analysis.

Samples were genotyped at 958,178 markers using the Illumina Infinium HumanOmniExpressExome array. Genotyped variants were QC'd, phased, and imputed based on the Phase 1 reference panel from the 1,000 Genomes Project. Variants with INFO < 0.8 or MAF < 0.05 were filtered out, and approximately 6.4 million variants were included in further analysis. Further details on processing of raw data, normalization, and quality control procedures, can be found in [2].

The R package MatrixEQTL [16] was used to fit an additive linear model between the expression of 16,423 genes and SNP dosage data at 6.4 million markers within a 1 Mb window around the transcription start site for each gene, including covariates for

diagnosis, five ancestry covariates and known and hidden variables detected by surrogate variable analysis.

Following eQTL identification, summary statistics on 72,441,005 SNPs and 15,791 autosomal genes were retained for downstream analyses. Overall, the model identified 2,154,331 significant cis-eQTL, (i.e., SNP–gene pairs within 1 Mb of a gene) at a false discovery rate (FDR) ≤ 5%, for 13,137 (80%) genes.

Methylation QTL (mQTL) analysis

For the mQTL dataset, we used pre-QC'd DNA methylation data and imputed genotypes on non-psychiatric adult Caucasian control donors (age > 13, N=121). We briefly summarize here the procedures to process the raw data. More details on data processing, normalization, and QC can be found in [6].

DNA methylation was assessed on postmortem tissue homogenates of the dorsolateral prefrontal cortex (DLPFC, Brodmann areas 9 and 46) on 534 unique subjects using the Illumina HumanMethylation450 ("450k") microarray (which measures CpG methylation across 473,058 probes covering 99% of RefSeq gene promoters). The average intensity was used to check for low quality samples, intensities from the sex chromosomes were used to drop samples that had predicted sex which was different from its recorded value, and across-sample quantile normalization was used. DNA for genotyping was obtained from the cerebella of samples with either the Illumina Human Hap 650v3, 1M Duo V3, or Omni 5M BeadArrays. Genotypes were called, QC'd, phased and imputed to the 1000 Genomes Phase 3 variant set, separately by genotyping platform. Imputed genotypes were then merged across the three platforms, and SNPs with MAF > 5% and

imputation quality above 90% were retained across the samples. Multidimensional scaling (MDS) components were obtained for quantitative measures of ancestry.

For the mQTL association analysis, we only considered 121 adult Caucasian individuals (age > 13). The analysis was conducted using the R package MatrixEQTL [16], fitting an additive linear model up to 20kb distance between each SNP and CpG analyzed, including as covariates the first five MDS components from the genetic data and the first 8 PCs (based on the 100,000 most inter-individual variable probes for computational efficiency). Summary statistics on 47,675,913 SNPs and 473,058 Illumina 450k probes were used for downstream analyses. Overall, the model identified 3,601,681 significant cis-mQTL, (i.e., SNP–probe pairs within 20kb distance of a probe) at a false discovery rate (FDR) ≤ 5%, for 127,237 (27%) probes.

Moloc Analysis

The GWAS, eQTL, mQTL datasets were filtered by minor allele frequency greater than 5% and had individually been filtered by imputation quality (Methods).. The Major Histocompatibility (MHC) region (chr 6: 25 Mb - 35 Mb) was excluded from all co-localization analyses due to the extensive linkage disequilibrium. We applied a genic-centric approach, defined *cis*-regions based on a 50kb upstream/downstream from the start/end of each gene, since our goal is to link risk variants with changes in gene expression. We evaluated all methylation probes overlapping the *cis*-region. The number of cis-regions/methylation pairs is higher than the count of genes because, on average, there are more than one methylation sites per gene. Common SNPs were evaluated in the colocalization analysis for each gene, and each methylation probe, and

GWAS. In total, 12,003 *cis*-regions and 481,995 unique *cis*-regions/methylation probes were tested. Genomic regions were analyzed only if greater than 50 SNPs were in common between all the datasets. Across all of the analyses, a posterior probability equal to, or greater than, 80% for each configuration was considered evidence of colocalization.

In order to compare existing methods for colocalization of two trait analyses with three traits, we applied *moloc* using the same region definitions across the same set of SNPs, using a previously developed method (coloc[11]). Effect sizes and variances were used as opposed to p-values, as this strategy achieves greater accuracy when working with imputed data[11].

Simulations

We simulated genotypes from sampling with replacement among haplotypes of SNPs with a minor allele frequency of at least 5% found in the phased 1000 Genomes Project within 49 genomic regions that have been associated with type 1 diabetes (T1D) susceptibility loci (excluding the major histocompatibility complex (MHC) as previously described[17]. These represent a range of region sizes and genomic topography that reflect typical GWAS hits in a complex trait. For each trait, two, or three “causal variants” were selected at random. We have simulated continuous traits, and assume that causal effect follow a multivariate Gaussian distribution, with each causal variant explaining 0.01 variance of the trait in the GWAS data, and 0.1 in the eQTL and mQTL datasets. For the null scenario, the causal variants explain zero variance of the traits. Each scenario was simulated 1,000 times. To quantify false positive rates on a large

number of tests, we simulated the null 500,000 times. We simulated the 15 possible scenarios with different sharing patterns between the GWAS, eQTL, and mQTL datasets. We used sample sizes of 82,315, 467, and 121 individuals to reflect our true sample sizes. We also used different combinations of sample sizes to explore power to detect the correct hypothesis.

We estimated the number of false positives within each simulated scenario, by counting the proportion of simulations under the null that passed a posterior probability supporting each of the 14 hypothesis at a particular threshold (PPA>=threshold). We also report the false positives using the sum of the posteriors (PPA.ab + PPA.abc + PPA.abc). The false positive rate is the number of false positives over 1,000 simulations. We repeated this procedure using 500,000 simulations under our true sample sizes.

We next sought to compare the misclassification rates, and power to detect the correct hypothesis. To compute the number of misclassified calls within each simulated scenario, we counted the proportion of simulations that passed a posterior probability supporting a different hypothesis from the one simulated at a particular threshold (PPA>=threshold). We estimated power to distinguish a particular hypothesis from the others by counting the proportion of simulations that did not reach a posterior probability supporting each scenario at a particular threshold (PPA(true)<threshold).

To explore the effect of linkage disequilibrium (LD) on estimated posterior probability, we first computed an LD score for each SNP in the region, defined as the sum of the squared correlation between a SNP and all the SNPs in the region. To assess the degree of LD at a locus we took the average of these scores.

All analyses were conducted in R.

RESULTS

Sample Size Requirements

We explored false positive rates and the posterior probability under different sample sizes. **Figure S1** illustrate the posterior probability distribution across all of the possible scenarios that includes three traits: GWAS, eQTL and mQTL. With a GWAS sample size of 10,000 and eQTL and mQTL sample sizes of 300, the method provides reliable evidence to detect a shared causal variant behind the GWAS and another trait (median posterior probability of any hypothesis >50%). Although in this paper we analyze GWAS, eQTL and mQTL, our method can be applied to any combinations of traits, including 2 GWAS traits and an eQTL dataset. We explored the minimum sample size required when analyzing two GWAS datasets (GWAS1, GWAS2) and one eQTL (**Figure S2**). The method provides reliable evidence for all hypotheses when the two GWAS sample sizes are 10,000 and eQTL sample size reaches 300. False positive rates are below 0.05 even if a threshold of 0.3 for posteriors is used, and where the causal variant is masked (**Tables S4**, **S5**, **S6**). When samples are greater than 10000 for GWAS and 300 for eQTL and mQTL, our misclassification rates are all below 0.05 (**Table S8**). Where the causal variant is masked, sample sizes need to reach 10000 for GWAS and 500 for eQTL and mQTL, for our misclassification rates to be below 0.05 (**Table S9**). Given the small sample size for the mQTL data, the algorithm has trouble detecting a different causal variant for the mQTL dataset (**Table S7**). For example, evidence pointing to two different causal variants between GWAS and eQTL could be generated by the presence of three causal variants in reality, but the causal variant for

mQTL remains undetected. For this reason, we focused on cases with shared casual variants between GWAS, eQTL, with or without mQTL.

It is instructive to observe where evidence for other hypotheses is distributed. **Figure 2** illustrates the accuracy of our approach under different scenarios where two or three causal variants are shared. For example, under simulations of one shared variant for GWAS and eQTL and a second variant for mQTL (GE.M), on average 60% of the evidence points to the simulated scenario, while 12% point to GE, 12% to G.E.M and 7.2% to GEM.

Choice of priors

The algorithm requires the definition of prior probabilities at the SNP level for the association with one (p1), two (p2), or three traits (p3). We set the prior probability that a variant is associated with one trait as 1×10^{-4} for GWAS, eQTL and mQTL, assuming that each genetic variant is equally likely a priori to affect gene expression or methylation or disease. This estimate has been suggested in the literature for GWAS[18] and used in similar methods[19]. We set the priors $p2 = 1 \times 10^{-6}$, $p3 = 1 \times 10^{-7}$ based on sensitivity and exploratory analysis of genome-wide enrichment of GWAS risk variants in eQTLs and mQTLs. In **Figure S3**, we find eQTLs and mQTLs to be similarly enriched in GWAS, justifying our choice of the same prior probability of association across the two traits. These values are also suggested by a crude approximation of *p2* and *p3* from the common genome-wide significant SNPs across the three dataset.

We performed sensitivity analyses using different priors. Specifically, we fixed p1 to $1x10^{-4}$ and tested a range of priors for p2 and p3 from $1x10^{-5}$ to $1x10^{-8}$, with increasing difference between p1, p2 and p3. We used a form of internal empirical calibration to compare our prior and posterior expectations. We considered a range of values for p2 and p3 while keeping p1 fixed, and find that the posterior expectation of colocalisation most closely resembled the prior expectation under our choice of priors (**Table S1**).
We note that our R package implementation allows users to specify a different set of priors.

Co-localization of eQTL, mQTL and risk for Schizophrenia

We applied our method to SCZ GWAS using eQTLs derived from 467 samples and mQTL from 121 individuals. Our aim is to identify the genes important for disease through colocalization of GWAS variants with changes in gene expression and DNA methylation. We analyzed associations genome-wide, and report results both across previously identified GWAS loci, and across potentially novel loci. While we consider all 15 possible scenarios of colocalization, here we focus on gene discovery due to higher power in our eQTL dataset, by considering the combined probabilities of cases where the same variant is shared across all three traits GWAS, eQTLs and mQTLs (GEM > 0.8) or scenarios where SCZ risk loci are shared with eQTL only (GE > 0.8 or GE.M > 0.8) (**Table 1**). We identified 1,053 cis-regions/methylation pairs with posterior probability above 0.8 that are associated with all three traits (GEM), or eQTLs alone (GE or GE.M). These biologically relevant scenarios affect overall 84 unique genes and

include 39 genes that fall within the previously identified SCZ LD blocks (**Table S2**) and 45 potentially novel genes outside of these regions (**Table S3**). Fifty-two out of the 84 candidate genes influence SCZ, gene expression and methylation (GEM>=0.8). One possible scenario is that the variants in these genes could be influencing the risk of SCZ through methylation, although other potential interpretations such as pleiotropy should be considered.

Addition of a third trait increases gene discovery

We examined whether moloc with 3 traits enhance power for GWAS and eQTL colocalization compared to using 2 traits. In simulations to compare coloc and moloc under one causal variant and our true sample sizes for all three datasets, we observe a fold increase of 1.5 for gene discovery using moloc versus coloc. Moloc with three traits recovers all the genes discovered using *coloc* with eQTL and mQTL, and additional genes from the inclusion of the third layer. In our real data, colocalization analysis of only GWAS and eQTL traits identified 45 genes with a posterior probability, PP4 in *coloc*, of >= 0.8. The 39 additional genes that were found by adding methylation include genes such as *CALN1,* a neuronal transcript associated with abnormalities in sensorimotor gating in humans[20], that would have been missed by only GWAS and eQTL colocalization.

Loci overlapping reported SCZ LD blocks

Psychiatric Genomics Consortium (PGC) identified 108 independent loci and annotated LD blocks around these, 104 of which are within non-HLA, autosomal regions

of the genome[10]. In **Table 1** we report the number of identified gene-methylation pairs and unique genes under each scenario that overlap the SCZ-associated LD blocks. Out of the 78 SCZ-associated LD blocks we examined in our analysis, we found colocalizations in 20 of them with an average gene density per block of 2.4 unique genes. **Figure 3A** illustrates the average distribution of the posteriors across these regions. Cumulatively, 12% of the evidence points to shared variation with an eQTL (GE, GE.M and GEM). The majority of the evidence within these regions (64%) did not reach support for shared variation across the three traits, with 20% not reaching evidence for association with any traits, and 44% with only one of the three traits (36% with GWAS; 6% with eQTL, 2% with mQTLs). The lack of evidence in these regions could be addressed with greater sample sizes. **Figure 3B** shows the evidence for colocalization of GWAS with eQTL or mQTL across the 39 candidate genes. We provide illustrative examples of SCZ association with expression and DNA methylation in the FURIN locus (**Figure 4** and **Figure S4A**).

Potentially novel SCZ loci

We found 45 unique genes that have a high posterior for SCZ and eQTL, but fall in regions not previously identified to be associated with SCZ (at p-value of 5×10^{-8}*).* All genes were far from a SCZ LD block (more than 150kb, **Table S3**), and contained SNPs with p-values for association with SCZ ranging from 10^{-4} to 10^{-8}. These genes will likely be identified using just the GWAS signal if the sample size is increased. *KCNN3* is among these genes which encodes an integral membrane protein that forms a voltage-independent calcium-activated channel. It regulates neuronal excitability by contributing

to the slow component of synaptic afterhyperpolarization[21]. A plot of the associations with the three datasets within this locus is shown in **Figure S4B.**

Comparison with previous findings

We compare our gene discovery results to previous studies that assess GWAS-eQTL[2–5] or GWAS-mQTL[5,7–9] colocalization using the same or similar datasets (**Table 2**). A substantial proportion of genes detected in our study (range 44%-85%) was validated with four studies [2–5] that used eQTL and GWAS integration to prioritize genes important for schizophrenia. Several studies have also linked methylation data with schizophrenia [7–9]. Two recent studies[7,9] used blood mQTL data from 639 samples and identified colocalization of SCZ loci with 32 and 200 methylation probes by applying COLOC and SMR, respectively. A substantial proportion of SCZ-mQTL colocalization was validated in our study (COLOC: 46%; SMR: 18%, **Table 2**). Another study[8] used mQTL data from 166 fetal brain samples and identified 297 methylation probes important for schizophrenia. We analyzed 184 of those and found evidence for 13 probes. We note that our methylation data did not included fetal brain samples. Finally, a recent study[5] identified 44 genes involved in schizophrenia through TWAS, followed by integration with chromatin data in blood that resulted in 11 genes associated with GWAS, eQTL and epigenome QTL. We analyzed 8 out of the 11 associations and confirmed 6 of these genes that, in our study, influence SCZ through eQTL and mQTL.

Association of gene expression with methylation

We explored direction of effects of methylation and expression, for gene

expression and DNA methylation that colocalize (PPA.GEM + PPA.EM + PPA.G.EM >= 0.8). Overall, we tested 1,947 DNA methylation and gene expression pairwise interactions and found a significant negative correlation between the effect sizes of methylation and expression in the proximity of the transcription start site (**Figure 5**, p-value:<2.2e-16).

DISCUSSION

In this paper, we propose a statistical method for integrating genetic data from molecular quantitative trait loci (QTL) mapping into genome-wide genetic association analysis of complex traits. The proposed approach requires only summary-level statistics and provides evidence of colocalization of their association signals. To our knowledge, a method integrating more than two traits is lacking. In contrast to other methods that attempt to estimate the true genetic correlation between traits such as LD score regression[22] and TWAS[23], *moloc* focuses on genes that are detectable from the datasets at hand. Thus, if the studies are underpowered, most of the evidence will lie in the null scenarios. We note that our model is the same as *gwas-pw* in Pickrell et al.[13] under specific settings. Precisely, *gwas-pw* averages over Bayes factors computed with W = 0.01, W = 0.1, and W = 0.5 (Methods). We provide this as an option that can be specified by the user. Additionally, *gwas-pw* estimates the prior parameters genome-wide using a maximization procedure. However, we note that, unlike *gwas-pw* that focuses on genome-wide estimation across pairs of traits, our approach focuses on one locus at a time with multiple traits.

We expose one possible application of this approach in SCZ. In this application, we focus on scenarios involving eQTLs and GWAS, alone or in combination with mQTLs. Other scenarios are also biologically important. For example, colocalization of GWAS and mQTL excluding eQTLs (GM.E scenario) could unveil important methylation mechanisms affecting disease but not directly influencing gene expression in *cis*. We report these and other scenarios in our web resource and encourage further examination of these cases in future analyses. The GEM scenario provides evidence

that SCZ risk association is mediated through changes in DNA methylation and gene expression. While our method does not detect causal relationships among the associated traits, i.e. whether risk allele leads to changes in gene expression through methylation changes or vice versa, there is evidence supporting the notion that risk alleles might affect transcription factor binding and epigenome regulation that drives downstream alterations in gene expression[24,25]. Importantly, our method helps to link a specific gene to a methylation probe. DNA methylation is one the best studied epigenetic modifications. Methylation can alter gene expression by disrupting transcription factor binding sites (with variable consequences to expression depending on the TF), or by attracting methyl-binding proteins that initiate chromatin compaction and gene silencing. Therefore methylation can be associated with both increased or decreased gene expression[24,26]. Increased CpG methylation in promoter regions is usually associated with silencing of gene expression[27]. However, in genome-wide expression and methylation studies, the correlation of methylation and gene expression is low or the pattern of association is mixed, even for CpG methylation within promoter regions[26]. We found a negative correlation between the effect sizes of methylation and expression in the proximity of the transcription start site. However, we note that the current assay (Illumina 450K) cannot discriminate DNA methylation from hydroxymethylation sites. DNA methylation is generally associated with the inhibition of gene expression, while DNA hydroxymethylation, the oxidized form of methylation, has been associated with enhancers and increased gene expression.

We provide posterior probabilities supporting respective hypotheses for each gene-methylation pair analyzed, and the SNP for each trait with the highest probability

of colocalization with any other trait. For example, the SNP with the highest posterior probability of GWAS colocalization with eQTL or mQTL will be computed from PPA of GE + GE.M + GM + GM.E + GEM. However, the aim of this method is not fine-mapping of SNPs and we encourage researchers to further analyze the identified local associations with methods better suited for fine-mapping.

We assign a prior probability that a SNP is associated with one trait (1×10^{-4}), to two (1×10^{-6}), and to three traits (1×10^{-7}). We find support for our choice of priors in the data using two methods. The first uses stratified QQ plots (Figure S3). We find that eQTL enrichment in GWAS has a similar enrichment to mQTL in GWAS. The second is a form of empirical calibration as in Guo et al.[28]. We find that the prior and posterior expectations of colocalisation matched more closely under our choice of priors (Figure S6). However the choices for prior beliefs for each hypothesis are always arguable. One could estimate priors for the different combinations of datasets. Pickrell et al.[13] proposed estimation of enrichment parameters from genome-wide results maximizing *a posteriori* estimates for two traits. For multiple traits, another possibility is using deterministic approximation of posteriors[29]. We leave these explorations to future research.

The results of this analysis apply to a particular brain region (dorsolateral prefrontal cortex), age period (adulthood), and ancestry (Caucasians only). We justify using functional data from DLPFC to examine the colocalization with schizophrenia variants as it is the most proximal to disease etiopathogenesis tissue [4,5]. In addition, due to the tissue specificity of gene expression regulatory mechanisms, we matched eQTL and mQTL data on the same brain region and age period. The genotypes and gene expression data reported by the CommonMind Consortium (CMC) comprises the largest

existing postmortem brain genomic resource from individuals with psychiatric disorders as well as unaffected controls. The mQTL dataset used here is the largest dataset in the adult brain measured in the brain region and age period considered. Although this was out of the scope of this paper, we encourage application of similar methods to functional data derived from different tissues and age periods to elucidate the spatiotemporal regulatory mechanisms of gene expression that are involved in the etiopathogenesis of schizophrenia.

The method makes use of LD to weigh out the posteriors for the different models, therefore the statistics (priors and posteriors of configurations) will depend on the pattern of association (LD) and the number of SNPs in the region (Q). Specifically, increased LD in a region with one causal variant in the decreases our chance to detect a shared causal effect (**Figure S5A**). This is because in loci where the extent of LD is strong (a large number of variants with the same strength of association), there is uncertainty on whether we are dealing with a single variant causal for both traits, or two independent variants in the same LD block. Similarly, the chance of the same SNP being causal for all three traits decreases as Q increases (**Figure S5B**).

The Bayes Factors under the models of colocalization (for the case of a single variant affecting more than one trait) are computed by multiplying the individual WABFs together, and this assumes independence of the effect sizes for the traits. Independence is appropriate in the case of analyzing different phenotypes, or eQTLs in different tissues. On the other hand, this assumption may be inappropriate in other cases, for example if we were looking at colocalization of a variant for the same trait in two different studies, or the same eQTLs across different tissue type, or the same trait

in two different studies. A more general BF computation which includes cases where the effects are correlated has been proposed in [15] and could be used to extend our approach to these situations. Additionally, correlation among the SNP effect sizes may result if the studies contain overlapping individuals. In this case we may overestimate the evidence in favor of colocalization. We could adjust SNP Bayes factors to account for this overlap as in [14]. The datasets we used in the current analysis does not contain overlapping individuals, however we provide the code to use this approach.

We note that this approach can be extended to more than three traits. Since the calculations are analytical and no recursive method is used, computation time for a region with 1000 SNPs is less than one second. However, time increases exponentially as number of traits increases. For four traits it is about 3 seconds, for five traits it is greater than 22 minutes.

Overall, owing to the increasing availability of summary statistics from multiple datasets, the systematic application of this approach can provide clues into the molecular mechanisms underlying GWAS signals and how regulatory variants influence complex diseases.

CONFLICTS OF INTEREST

None reported.

SUPPLEMENTAL DATA

Supplemental Data include four figures and four tables.

CONSORTIA

The CommonMind Consortium includes: Menachem Fromer, Panos Roussos, Solveig K Sieberts, Jessica S Johnson, Douglas M Ruderfer, Hardik R Shah, Lambertus L Klei, Kristen K Dang, Thanneer M Perumal, Benjamin A Logsdon, Milind C Mahajan, Lara M Mangravite, Hiroyoshi Toyoshiba, Raquel E Gur, Chang-Gyu Hahn, Eric Schadt, David A Lewis, Vahram Haroutunian, Mette A Peters, Barbara K Lipska, Joseph D Buxbaum, Keisuke Hirai, Enrico Domenici, Bernie Devlin, Pamela Sklar

ACKNOWLEDGMENTS

We would like to thank Chris Wallace at the Department of Medicine and MRC Biostatistics Unit, Cambridge Biomedical Campus, University of Cambridge, Cambridge, UK.

This work was supported by the National Institutes of Health (R01AG050986 Roussos and R01MH109677 Roussos), Brain Behavior Research Foundation (20540 Roussos), Alzheimer's Association (NIRG-340998 Roussos) and the Veterans Affairs (Merit grant BX002395 Roussos). Additionally, this work was supported in part through the computational resources and staff expertise provided by Scientific Computing at the Icahn School of Medicine at Mount Sinai.

Data were generated as part of the CommonMind Consortium supported by funding from Takeda Pharmaceuticals Company Limited, F. Hoffman-La Roche Ltd and NIH grants R01MH085542, R01MH093725, P50MH066392, P50MH080405, R01MH097276, RO1-MH-075916, P50M096891, P50MH084053S1, R37MH057881 and R37MH057881S1, HHSN271201300031C, AG02219, AG05138 and MH06692. Brain tissue for the study was obtained from the following brain bank collections: the

Mount Sinai NIH Brain and Tissue Repository, the University of Pennsylvania Alzheimer's Disease Core Center, the University of Pittsburgh NeuroBioBank and Brain and Tissue Repositories and the NIMH Human Brain Collection Core. CMC Leadership: Pamela Sklar, Joseph Buxbaum (Icahn School of Medicine at Mount Sinai), Bernie Devlin, David Lewis (University of Pittsburgh), Raquel Gur, Chang-Gyu Hahn (University of Pennsylvania), Keisuke Hirai, Hiroyoshi Toyoshiba (Takeda Pharmaceuticals Company Limited), Enrico Domenici, Laurent Essioux (F. Hoffman-La Roche Ltd), Lara Mangravite, Mette Peters (Sage Bionetworks), Thomas Lehner, Barbara Lipska (NIMH).

WEB RESOURCES

We developed a web site to visualize the colocalization results of SCZ GWAS, eQTL, mQTLs under all possible scenarios (**icahn.mssm.edu/moloc**). The browser allows searches by gene, methylation probe, and scenario of interest. The *moloc* method is available as an R package from https://github.com/clagiamba/moloc.

FIGURE TITLES AND LEGENDS

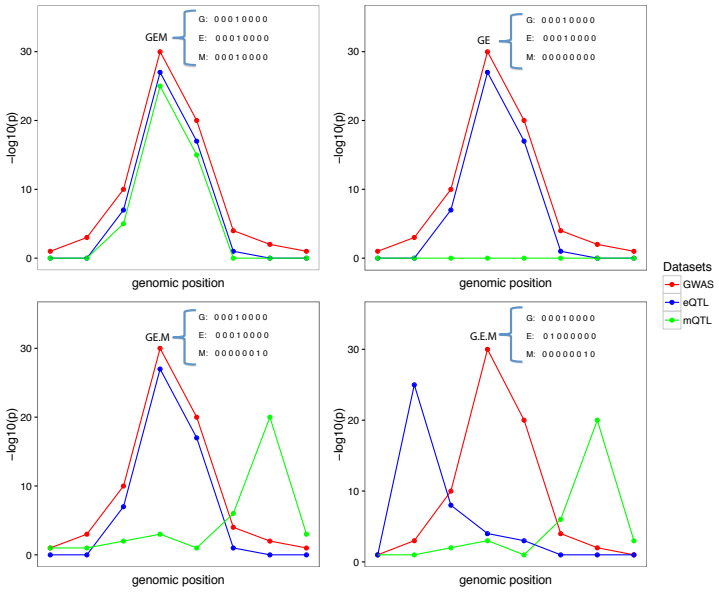

Figure 1. Graphical representation of four possible configurations at a locus with 8 SNPs in common across three traits. The traits are labeled as G, E, M representing GWAS (G), eQTL (E), and mQTL (M) datasets, respectively. Each plot represents one possible configuration, which is a possible combination of 3 sets of binary vectors indicating whether the variant is associated with the selected trait. Left plot top panel (GEM scenario): points to one causal variant behind all of the associations; Right plot top panel (GE scenario): represent the scenario with the same causal variant behind the GE and no association or lack of power for the M association; Left plot bottom panel (GE.M scenario): represents the case with two causal variants, one shared by the G and E, and a different causal variant for M; Right plot bottom panel (G.E.M. scenario): represents the case of three distinct causal variants behind each of the datasets considered.

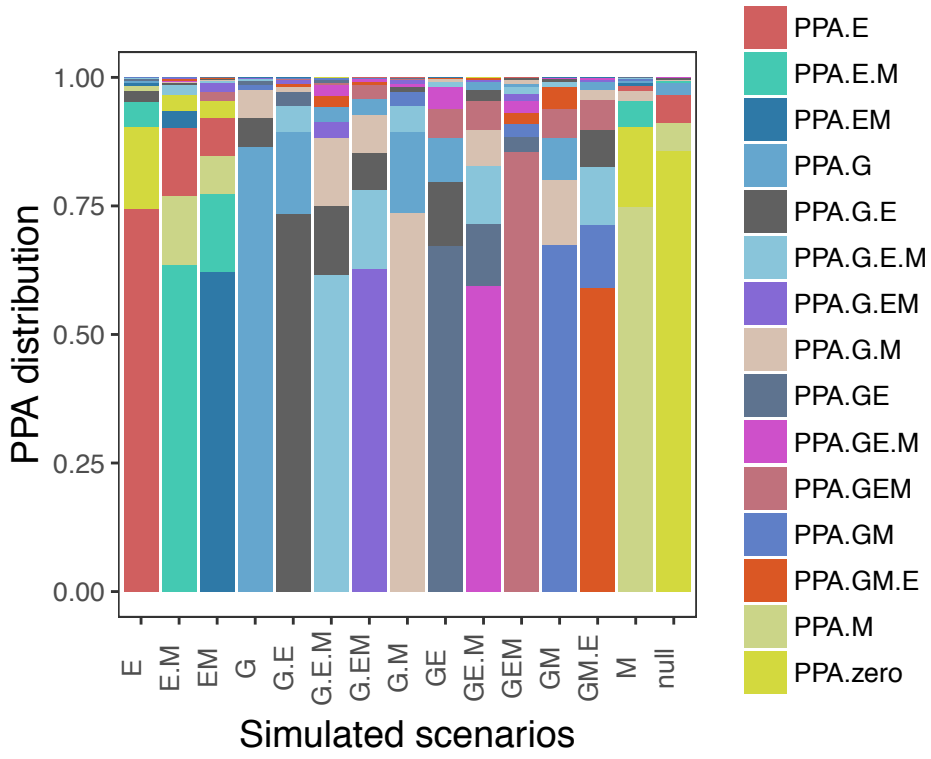

Figure 2. Results from simulations under colocalization/non-colocalization scenarios using a sample size of 10,000 individuals for GWAS trait (denoted as G), 300 for eQTL trait (denoted as E), and 300 for mQTL trait (denoted as M). X-axis shows all 15 simulated scenarios, e.g. G.E.M, three different causal variants for each of the three traits; G.EM, 2 different causal variants, one for G and one shared between E and M; GE, 1 shared causal variant for G and E; GE.M, 2 different causal variants, one shared between G and E and one for M; GEM, one causal variant shared between all the three traits. Y-axis shows the distribution of posterior probabilities under the simulated scenario. The height of the bar represents the mean of the PPA for each configuration across simulations.

A

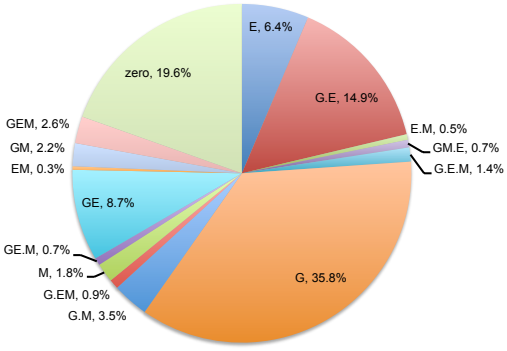

B

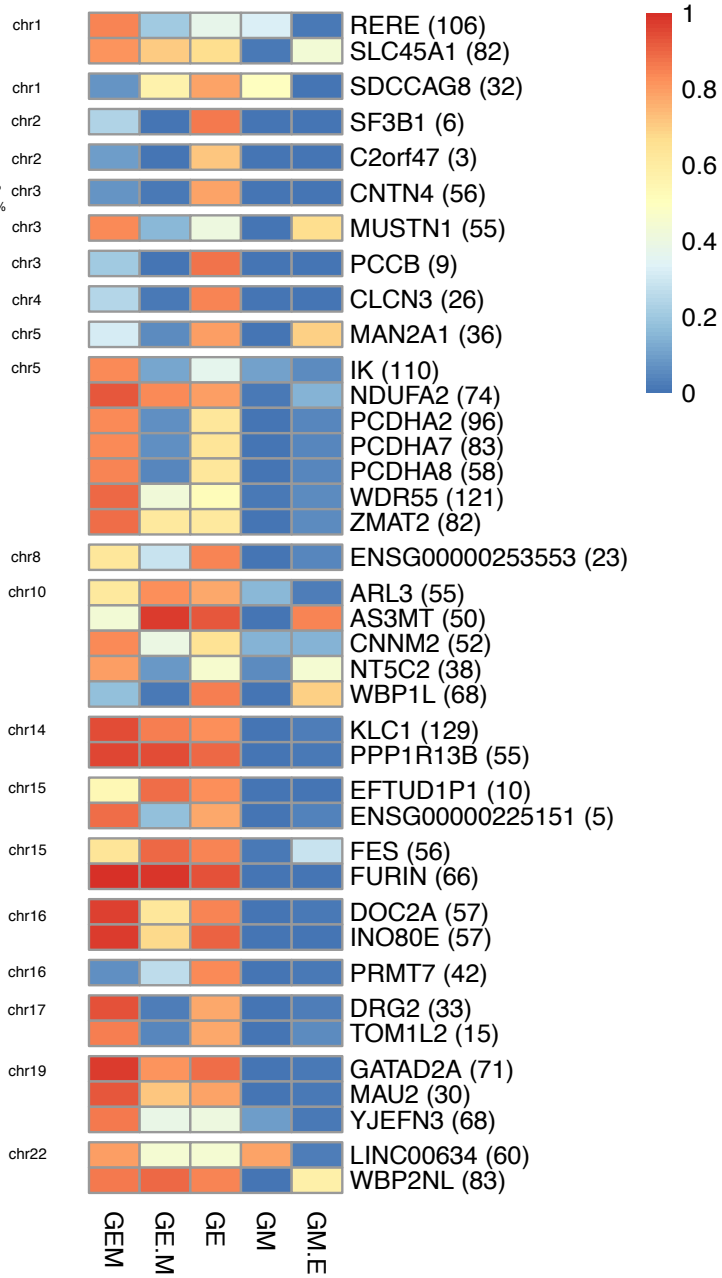

Figure 3. Summary of genes identified using three-trait colocalization within the SCZ LD blocks. **A**. Mean posterior probability for each hypotheses computed using the cis-regions overlapping the SCZ LD blocks. Sections of the pie chart represent the 15 scenarios representing the possible combination of the three traits. The "." between the traits denotes scenarios supporting different causal variants. The combined scenarios GE, GE.M, GE account for 12.0%. **B**. Heatmap displaying the maximum posterior probabilities reached by the 39 regions overlapping known SCZ LD blocks (gene, number of methylation probes).

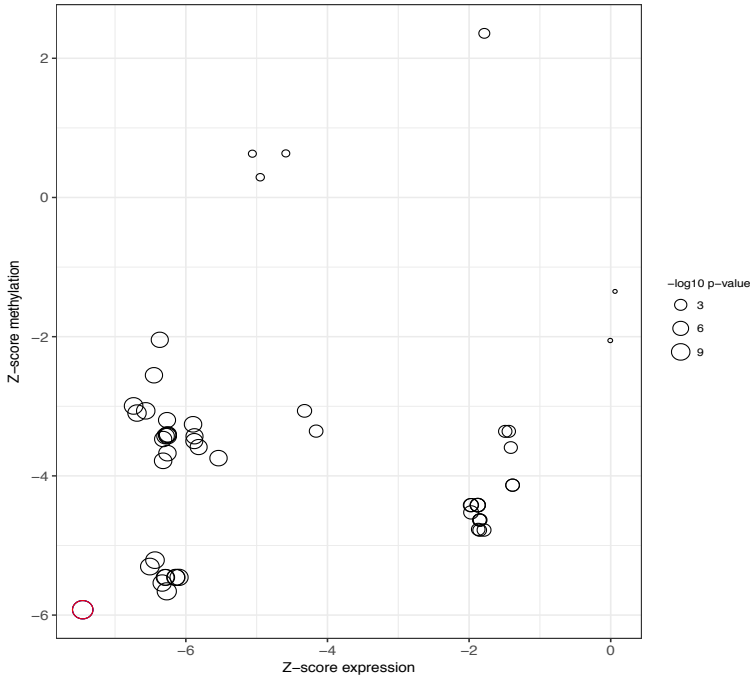

Figure 4. Illustration of one example of colocalization results with GWAS-eQTL-mQTL. *FURIN* gene and cg24888049; Shown are Z-scores (regression coefficients/standard errors) from association of expression (x-axis) and association of methylation (y-axis) at the *FURIN* locus. Each point represents a SNP and the size of the dot represent the

level of association using Z-scores. The red point shows the SNP with the strongest evidence for eQTL, mQTL, GWAS (rs4702).

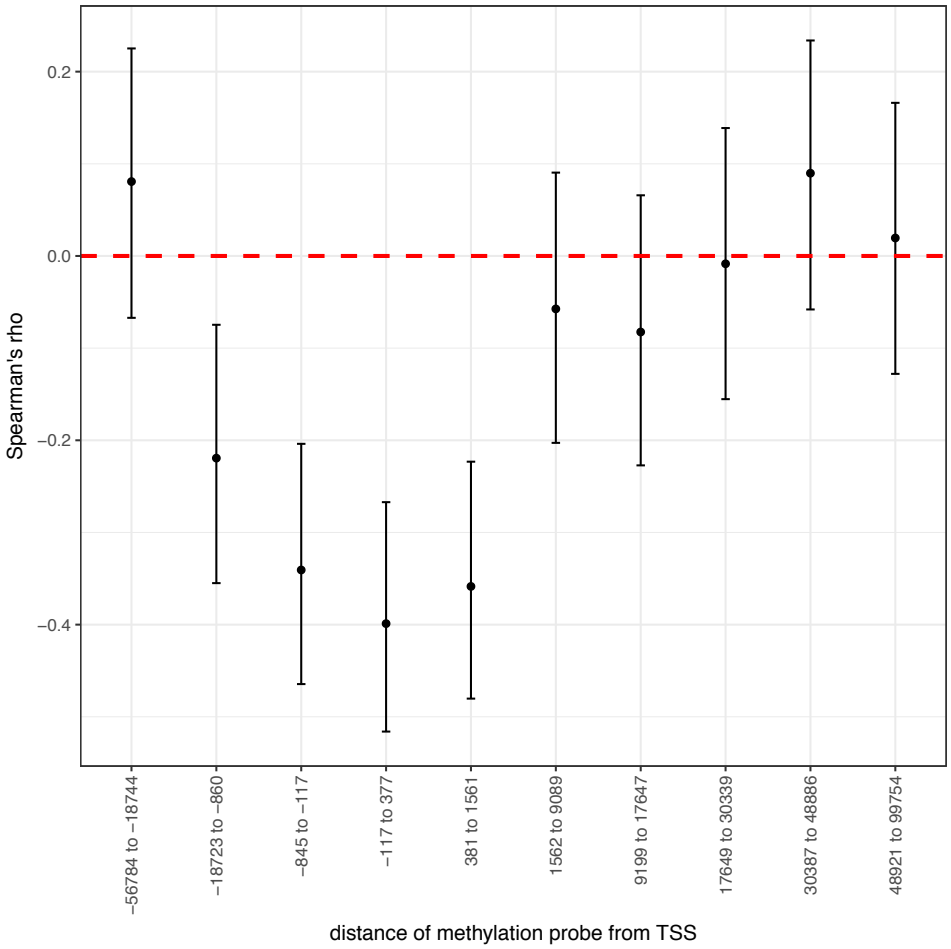

Figure 5. Spearman correlation of eQTL and mQTL effect estimates by distance from transcription start site of the gene. Intervals of methylation probe distance from TSS were estimated based on 10 equal size bins.

TABLE TITLES AND LEGENDS

Table 1. Number of genes with evidence of colocalization (PPA>=0.8) under each scenario.

Scenarios	Sharing of variant	Unique gene-methylation pairs	Unique genes		
		Total PPA>=80%	Total PPA>=80%	Overlapping SCZ LD blocks	Number of LD blocks
Null	No associations	268569	9317	90	55
G	GWAS only	4331	215	146	63
E	eQTL only	97852	3597	14	12
M	mQTL only	21914	5588	42	28
G.E	GWAS not eQTL (2 causals)	1257	66	47	27
E.M	eQTL not mQTL (2 causals)	7542	1952	7	6
G.M	GWAS not mQTL (2 causals)	219	75	52	26
GE	GWAS,eQTL	359	30	18	14
EM	eQTL,mQTL	1494	769	3	3
GM	GWAS,mQTL	38	23	18	10
GM.E	GWAS,mQTL not eQTL (2 causals)	20	11	7	5
G.EM	eQTL,mQTL not GWAS (2 causals)	22	10	7	4
GE.M	GWAS,eQTL not mQTL (2 causals)	31	17	10	7
G.E.M	not GWAS not eQTL not mQTL (3 causals)	63	29	23	15
GEM	GWAS,eQTL,mQTL	123	52	25	11
GEM *or* GE.M *or* GE	**combined scenarios for GWAS,eQTL**	1053	84	39	20
total	total	481995	12003	273	78

Table 2. Summary of Previous Findings integrating SCZ GWAS, CMC eQTL and methylation datasets.

Reference	Fromer et al. [2]	Zhu et al. [3]	Hauberg et al. [4]	Gusev at al. [5]	Hannon et al. [7]	Hannon et al. [8]	Hannon [9] et al.
Method Used	**Sherlock**	**SMR**	**SMR**	**TWAS**	**COLOC**	**COLOC**	**SMR**
Datasets	GWAS SCZ (N=82315); eQTL in brain (N=537)	GWAS SCZ (N=82315); eQTL in blood (N=5311)	GWAS SCZ (N=82315); eQTL in brain (N=467)	GWAS SCZ (N=82315); eQTL in brain (N=621); chromatin QTL in blood (N=45)	GWAS SCZ (N=82315); mQTL in blood (N=639)	GWAS SCZ (N=82315); mQTL in fetal brain (N=166)	GWAS SCZ (N=82315); mQTL in blood (N=639)
Scenarios examined in our analysis	**22**	**9**	26	GWAS+eQTL**: 35** GWAS+eQTL+mQTL**: 8**	**15**	184	49
Validated scenarios (%) at PPA 0.8	**15 (68%)**	**4 (44.4%)**	**22 (85%)**	GWAS+eQTL**: 21 (60%)** GWAS+eQTL+mQTL**: 6 (75%)**	**7 (46%)**	**13 (7%)**	**9 (18%)**
Genes and methylation sites validated*	**GWAS+eQTL***: SF3B1, C2orf47, CNTN4, CLCN3, ENSG00000253553, PPP1R13B, EFTUD1P1, ENSG00000225151, FURIN, INO80E, TOM1L2, DRG2, MAU2, GATAD2A, WBP2NL*	**GWAS+eQTL**: *SF3B1, PCCB, C17ORF39, IRF3*	**GWAS+eQTL***: AL022476.2, ALMS1P, CLCN3, DOC2A, DRG2, EFTUD1P1, ELAC2, EMB, FAM86B3P, FURIN, GATAD2A, GOLGA2P7, INO80E, JRK, PCCB, PCDHA7, RBBP5, RP11-45P15.4, SF3B1, SLC9B1, SLCO4C1, VPS37A*	**GWAS+eQTL:** *ALMS1P ,C2orf47, CPNE7, DOC2A, DRG2, ELOVL7, EMB, FURIN, GATAD2A, MAU2, MCHR1, NDUFA2, NT5C2, PCCB, PCDHA2, PRMT7, SEPT10, SF3B1, SLC45A1, TMEM81, ZMAT2* **GWAS+eQTL+mQTL***: SLC45A1,PCCB,NDUFA2,PCDHA2,ZMAT2,PRMT7*	**GWAS+mQTL:** *cg00585072, cg01262667, cg02951883, cg08607108, cg08607108, cg08772003, cg19624444, cg26732615*	**GWAS+mQTL***: cg08772003, cg19624444, cg08607108, cg02951883, cg00585072, cg26732615, cg02206767, cg26395211, cg25066665, cg04140906, cg04398451, cg10596483, cg24634471*	**GWAS+mQTL***: cg25066665, cg02951883, cg07143303, cg08772003, cg14047540, cg04140906, cg12863693, cg04398451, cg26732615*

* Genes validated (GWAS+eQTL+mQTL and GWAS+eQTL) include the genes with PPA.GEM+PPA.GE+PPA.GE.M>= 80%; methylation sites validated (GWAS+mQTL) include PPA.GEM+PPA.GM+PPA.GM.E>= 80%.

REFERENCES

1. Visscher, P.M., Brown, M.A., McCarthy, M.I., and Yang, J. (2012). Five Years of GWAS Discovery. Am. J. Hum. Genet. *90*, 7–24.

2. Fromer, M., Roussos, P., Sieberts, S.K., Johnson, J.S., Kavanagh, D.H., Perumal, T.M., Ruderfer, D.M., Oh, E.C., Topol, A., Shah, H.R., et al. (2016). Gene expression elucidates functional impact of polygenic risk for schizophrenia. Nat. Neurosci. *19*, 1442–1453.

3. Zhu, Z., Zhang, F., Hu, H., Bakshi, A., Robinson, M.R., Powell, J.E., Montgomery, G.W., Goddard, M.E., Wray, N.R., Visscher, P.M., et al. (2016). Integration of summary data from GWAS and eQTL studies predicts complex trait gene targets. Nat. Genet. *48*, 481–487.

4. Hauberg, M.E., Zhang, W., Giambartolomei, C., Franzén, O., Morris, D.L., Vyse, T.J., Ruusalepp, A., Sklar, P., Schadt, E.E., Björkegren, J.L.M., et al. (2017). Large-Scale Identification of Common Trait and Disease Variants Affecting Gene Expression. Am. J. Hum. Genet. *100*, 885–894.

5. Gusev, A., Mancuso, N., Finucane, H.K., Reshef, Y., Song, L., Safi, A., Oh, E., O ’donovan, M.C., Katsanis, N., Crawford, G.E., et al. TITLE: Transcriptome-wide association study of schizophrenia and chromatin activity yields mechanistic disease insights.

6. Jaffe, A.E., Gao, Y., Deep-Soboslay, A., Tao, R., Hyde, T.M., Weinberger, D.R., and Kleinman, J.E. (2016). Mapping DNA methylation across development, genotype and schizophrenia in the human frontal cortex. Nat. Neurosci. *19*, 40–47.

7. Hannon, E., Dempster, E., Viana, J., Burrage, J., Smith, A.R., Macdonald, R., St

Clair, D., Mustard, C., Breen, G., Therman, S., et al. (2016). An integrated genetic-epigenetic analysis of schizophrenia: evidence for co-localization of genetic associations and differential DNA methylation. Genome Biol. *17*, 176.

8. Hannon, E., Spiers, H., Viana, J., Pidsley, R., Burrage, J., Murphy, T.M., Troakes, C., Turecki, G., O'Donovan, M.C., Schalkwyk, L.C., et al. (2016). Methylation QTLs in the developing brain and their enrichment in schizophrenia risk loci. Nat. Neurosci. *19*, 48–54.

9. Hannon, E., Weedon, M., Bray, N., O'Donovan, M., and Mill, J. (2017). Pleiotropic Effects of Trait-Associated Genetic Variation on DNA Methylation: Utility for Refining GWAS Loci. Am. J. Hum. Genet. *100*, 954–959.

10. of the Psychiatric Genomics Consortium, S.W.G. (2014). Biological insights from 108 schizophrenia-associated genetic loci. Nature *511*, 421–427.

11. Giambartolomei, C., Vukcevic, D., Schadt, E.E., Franke, L., Hingorani, A.D., Wallace, C., and Plagnol, V. (2014). Bayesian test for colocalisation between pairs of genetic association studies using summary statistics. PLoS Genet. *10*, e1004383.

12. Wakefield, J. (2009). Bayes factors for genome-wide association studies: comparison with P-values. Genet. Epidemiol. *33*, 79–86.

13. Pickrell, J.K., Berisa, T., Liu, J.Z., Ségurel, L., Tung, J.Y., and Hinds, D.A. (2016). Detection and interpretation of shared genetic influences on 42 human traits. Nat. Genet. *48*, 709–717.

14. Pickrell, J.K. (2014). Joint analysis of functional genomic data and genome-wide association studies of 18 human traits. Am. J. Hum. Genet. *94*, 559–573.

15. Wen, X., and Stephens, M. (2011). Bayesian methods for genetic association

analysis with heterogeneous subgroups: From meta-analyses to gene-environment interactions.

16. Shabalin, A.A. (2012). Matrix eQTL: ultra fast eQTL analysis via large matrix operations. Bioinformatics *28*, 1353–1358.

17. Wallace, C. (2013). Statistical testing of shared genetic control for potentially related traits. Genet. Epidemiol. *37*, 802–813.

18. Stephens, M., and Balding, D.J. (2009). Bayesian statistical methods for genetic association studies. Nat. Rev. Genet. *10*, 681–690.

19. Hormozdiari, F., van de Bunt, M., Segrè, A.V., Li, X., Joo, J.W.J., Bilow, M., Sul, J.H., Sankararaman, S., Pasaniuc, B., and Eskin, E. (2016). Colocalization of GWAS and eQTL Signals Detects Target Genes. Am. J. Hum. Genet. *99*, 1245–1260.

20. Roussos, P., Giakoumaki, S.G., Zouraraki, C., Fullard, J.F., Karagiorga, V.-E., Tsapakis, E.-M., Petraki, Z., Siever, L.J., Lencz, T., Malhotra, A., et al. (2016). The Relationship of Common Risk Variants and Polygenic Risk for Schizophrenia to Sensorimotor Gating. Biol. Psychiatry *79*, 988–996.

21. Deignan, J., Luján, R., Bond, C., Riegel, A., Watanabe, M., Williams, J.T., Maylie, J., and Adelman, J.P. (2012). SK2 and SK3 expression differentially affect firing frequency and precision in dopamine neurons. Neuroscience *217*, 67–76.

22. Bulik-Sullivan, B., Finucane, H.K., Anttila, V., Gusev, A., Day, F.R., Loh, P.-R., Duncan, L., Perry, J.R.B., Patterson, N., Robinson, E.B., et al. (2015). An atlas of genetic correlations across human diseases and traits. Nat. Genet. *47*, 1236–1241.

23. Gusev, A., Ko, A., Shi, H., Bhatia, G., Chung, W., Penninx, B.W.J.H., Jansen, R., de Geus, E.J.C., Boomsma, D.I., Wright, F.A., et al. (2016). Integrative approaches for

large-scale transcriptome-wide association studies. Nat. Genet. *48*, 245–252.

24. Tak, Y.G., and Farnham, P.J. (2015). Making sense of GWAS: using epigenomics and genome engineering to understand the functional relevance of SNPs in non-coding regions of the human genome. Epigenetics Chromatin *8*, 57.

25. Li, Y.I., Van De Geijn, B., Raj, A., Knowles, D.A., Petti, A.A., Golan, D., Gilad, Y., and Pritchard, J.K. RNA splicing is a primary link between genetic variation and disease.

26. Wagner, J.R., Busche, S., Ge, B., Kwan, T., Pastinen, T., and Blanchette, M. (2014). The relationship between DNA methylation, genetic and expression inter-individual variation in untransformed human fibroblasts. Genome Biol. *15*, R37.

27. Du, X., Han, L., Guo, A.-Y., and Zhao, Z. (2012). Features of methylation and gene expression in the promoter-associated CpG islands using human methylome data. Comp. Funct. Genomics *2012*, 598987.

28. Guo, H., Fortune, M.D., Burren, O.S., Schofield, E., Todd, J. a, and Wallace, C. (2015). Integration of disease association and eQTL data using a Bayesian colocalisation approach highlights six candidate causal genes in immune-mediated diseases. Hum. Mol. Genet. *24*, 3305–3313.

29. Wen, X., Pique-Regi, R., and Luca, F. (2017). Integrating molecular QTL data into genome-wide genetic association analysis: Probabilistic assessment of enrichment and colocalization. PLoS Genet. *13*.